Robotica (2021), **39**, pp. 2333–2348
doi:10.1017/S0263574721000345

CAMBRIDGE UNIVERSITY PRESS

RESEARCH ARTICLE

Computational efficiency of multi-body systems dynamic models

Cs. Antonya and R. G. Boboc*

Transilvania University of Brasov, 29 Eroilor, 500036 Brasov, Romania
*Corresponding author. Email: razvan.boboc@unitbv.ro

Received: 10 September 2019; **Revised:** 9 January 2021; **Accepted:** 10 March 2021; **First published online:** 16 June 2021

Keywords: multi-body systems; multi-particle systems; dynamics; computational efficiency

Abstract

For several decades, simulation and analysis of mechanisms have been performed with dedicated computer-aided engineering software that implements general dynamic formulations, known in the literature as multi-body systems (MBS) formulations. The MBS name is related to the structure of the mechanism, which is often considered to be a collection of bodies interconnected by mechanical joints (pairs). Nevertheless, only a few formulations are really based on a true multi-body mechanical model, while many others instantiate mathematically quite different mechanical concepts. This paper aims to identify and discuss the mechanical models that fundament the main multi-body mathematical formulations known in the literature. The main features of each model are outlined, based on a detailed presentation of the structure and equations of motion, together with their link with the kinematic and dynamic formulations. A comparative study related to computational efficiency is then presented for the identified main models, based on a test mechanism. Comparative advantages and disadvantages are discussed at the end, considering the identified mechanical models.

1. Introduction

In the last quarter century, multi-body systems (MBS) simulation technology evolved in powerful computer-aided engineering, analysis, and control software, which became widely used, complementing the finite element method especially when systems with large translational and rotational displacement in space are to be simulated [1]. The need to perform evaluations and verifications in engineering design has increased the emphasis given to simulation activities in industry, research, and development. The commercially available MBS codes include nowadays a wide range of services, allowing the simulation of sophisticated experiments with virtual prototypes of mechanical systems. The "MBS" name is related to the structure of the mechanical system, often regarded as a collection of bodies interconnected through joints. Nevertheless, only a few formulations are really based on a true MBS mechanical model (i.e., a set of interconnected bodies [1, 2, 3, 4, 5]), while others describe mathematically different mechanical models (e.g., a set of interconnected kinematic chains [6, 7, 8] or a set of interconnected particles [9, 10, 11]).

This paper presents a classification of the main formulations of the kinematics and dynamics of MBS and a comparative study of their computational efficiency. Previous classifications mentioned in the literature usually consider the types of coordinates involved [12]. The research focus is on four main approaches, namely "reference point coordinates," [2, 13, 14] "relative coordinates," [15] "natural coordinates," [16, 17] and particle-based formulations [9, 10, 11, 18]. Furthermore, in this paper, we associate mechanical models to these formulations and four distinctive classes of models were identified.

The differences between various models originate in the way the mechanical system is discretized and the types of entities that are used for this purpose (Fig. 1). Some formulations are built around the

© The Author(s), 2021. Published by Cambridge University Press.

https://doi.org/10.1017/S0263574721000345 Published online by Cambridge University Press

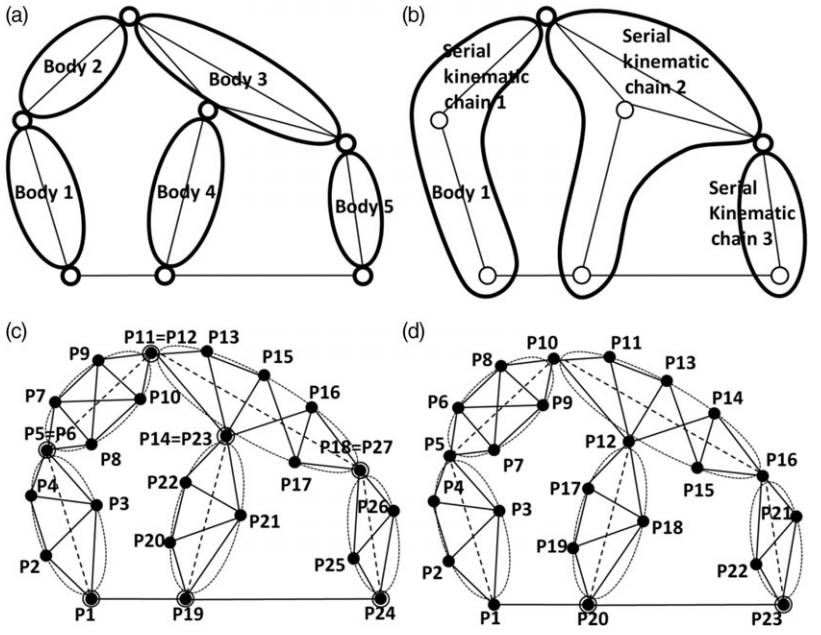


Figure 1. *Various mechanics-based models of an articulated mechanism (mechanical linkage). (a) multi-body system (MBS) model. (b) Kinematic chains of bodies (KCB) model. (c) Multi-particle system (MPS) model. (d) Kinematic chains of particles (KCP).*

mechanical concept of rigid body (Fig. 1(a), (b)), while others are based on the concept of mass particle (Fig. 1(c), (d)), as will be shown below. In both cases, there are models that take as a reference each individual entity and models that work with series (chains) of these entities. Hence, four main mechanical models can be distinguished: (i) MBS, (ii) kinematic chains of bodies (KCB), (iii) multi-particle system (MPS), and (iv) kinematic chains of particles (KCP).

Figure 1 shows various models of an articulated mechanism. The first type (Fig. 1(a)) is based on a true MBS representation, in which the linkage is regarded as a collection of independent rigid bodies that are interconnected through ideal joints. The second type of formulation is based on a representation that regards the mechanical linkage as a collection of KCB, interconnected through relative constraints (Fig. 1(b)). The third type regards the articulated mechanism as a collection of inter-constrained particles (Fig. 1(c)) and is called the MPS model [9, 10]. The fourth model (Fig. 1(d)) regards the mechanism as a set of KCP, interconnected through joints. The latter includes the natural coordinates formulation [9] as well as a pure particle-based formulation proposed in refs. [18, 19]. The following sections of this paper present the main features of each of the above model types, paying special attention to the structural formula and the meaning of its terms as well as the kinematic and dynamic formulations. Section 2 is dedicated to the multi-body formulation, Sections 3 and 4 to the serial kinematic chain formulations, and Section 5 to the multi-particle formulation. All model types and related formulations are exemplified for a test articulated mechanism and in Section 6 a comparative study is provided highlighting interesting structural features, advantages, and disadvantages for all models. Section 7 illustrates the results and discussion, and Section 8 presents the conclusions.

2. The MBS Model

The mechanism is mathematically described, according to this model, as a collection of bodies whose movement is subject to a set of absolute and relative motion constraints. This model has been used by many researchers since 1977 [2, 13, 14, 20]. Although MBS with perfect joints do not exist in reality,

https://doi.org/10.1017/S0263574721000345 Published online by Cambridge University Press

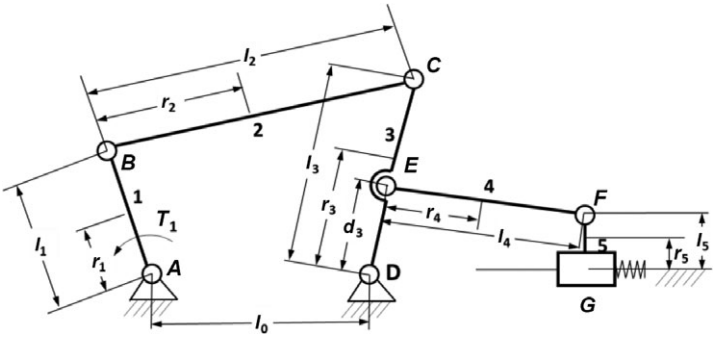


Figure 2. *Closed-loop test mechanism.*

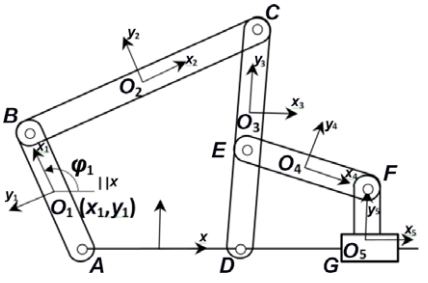


Figure 3. *The MBS model.*

[21] the models that fundament the multi-body formulations are defined in the context of idealized joints allowing a mobility analysis. As it will be shown later on in the paper, in our approach the mobility analysis is not only a mean to interpret the physical functionality of the system but also a first insight into the structure of the underlying mathematical model. Thus, for the MBS model, mobility is obtained by subtracting the number of ideal joint constraints from the degrees of freedom of all bodies (dof) considered as free bodies (Gruebler equation):

$$DOF = n \cdot S - \sum i \cdot C_i \tag{1}$$

in which n is the number of the mobile bodies, S is the motion dimension of the space (S=3 for planar and S=6 for the spatial mechanisms), and C_i is the number of joints of class i (the number of introduced constraints is defining the class).

This is the mechanical model that fundaments the Gruebler's formula, since it is the only model that operates with bodies and joints (constraints).

In the MBS model, each body is connected with a body-attached reference frame (BRF) defined by six independent generalized coordinates (three for the planar mechanisms). Most often these are the coordinates of the origin and the orientation angle with respect to the fixed reference frame.

The closed-loop test mechanism is presented in Fig. 2. The MBS model of this (Fig. 3) is characterized by $n \cdot S = 5 \cdot 3 = 15$ generalized coordinates q (q=[x_1,y_1,φ_1,x_2,… φ_5], where x_i and y_i are the coordinates of the BRF's origin O_i, i=1…5). However, in the mechanism context, not all the coordinates are independent due to the relative motion limitations introduced by the joints. Each of the relative motion constraints introduced by the physical connection in the mechanical joint is represented by mathematically written geometric conditions as algebraic equations that link the generalized coordinates of the neighboring bodies: a joint with dof=i introduces S-i algebraic equations.

A mechanism can be solved kinematically (solving only the algebraic equations), when the number of constraint equations, the joint constraint equations ($\Sigma i \cdot C_i$) together with the driving motions (M), equals the number of generalized coordinates. The first and second time derivatives of the constraint equations

https://doi.org/10.1017/S0263574721000345 Published online by Cambridge University Press

are leading up to the velocity and acceleration equations. The general expressions of the constraint equations at the displacement, velocity, and acceleration level are

$$\phi(\boldsymbol{q}, t) = 0, \dot{\phi}\,(\boldsymbol{q}, t) = 0, \ddot{\phi}\,(\boldsymbol{q}, t) = 0 \tag{2}$$

For the dynamic formulation, the total number of the equations of motion equals to the number of generalized coordinates plus the number of constraints. In this case, the number of independent coordinates is more complex to calculate since it depends if the mechanism has or does not have redundant constraints, which can be identified by investigating the rank of the Jacobian matrix of the constraint equations. Most usually for the entire mechanism, the differential equations with the general form are

$$[\boldsymbol{M}]\,[\ddot{\boldsymbol{q}}] - [\boldsymbol{J}]^T\,[\lambda] = \left[\boldsymbol{Q}_{ext}\right] \tag{3}$$

where M is the mass matrix, J is the constraints Jacobian matrix, λ is the Lagrange multipliers vector, and Q_{ext} is the vector of the generalized external forces.

The mass matrix M is constituted by simply assembling the individual body mass matrices on the diagonal of a system mass matrix ($\mathbf{M} = \text{diag}[m_1, m_1, I_1, m_2, \dots]$, m_i and I_i is the mass and moment of inertia of element i) the remaining elements of which are null. The term $[J]^T[\lambda]$ is the vector of the internal reaction forces, corresponding to the constraints represented in the Jacobian matrix. Numerous techniques to assembly these terms are provided in well-known textbooks [3, 4, 5, 7, 18]. The matrix form of the Newton–Euler equations (Eq. (2)) provides the simplest description of the equations of motion and is characteristic to numerous formulations known from the literature.

The test mechanism from Fig. 3 has five bodies connected by seven joints, with two geometric constraints algebraic equations for each. Thus, a number of 14 equations express the algebraic relations for the revolute joints $A, B, \dots, F$ and the translational joint G [12] as coincidence in the global reference frame of the coordinates of points on two adjacent bodies. Differentiating twice the constraint equations, the acceleration equations can be obtained in the form:

$$[\boldsymbol{J}]\,[\ddot{\boldsymbol{q}}] = -\left[\dot{\boldsymbol{J}}\right][\dot{\boldsymbol{q}}] - \frac{\partial}{\partial t}\left(\frac{\partial \Phi(\boldsymbol{q}, t)}{\partial t}\right) = [\boldsymbol{\psi}] \tag{4}$$

where J is the constraints Jacobian matrix.

J has two lines for each of the joints with dof = 1 (in total 14 lines) and 15 columns corresponding to the number of generalized coordinates (the elements of $\mathbf{q}$) and ψ has 14 lines:

$$[\mathbf{J}] = \begin{bmatrix} [\mathbf{J}_{1A}] & 0 & 0 & 0 & 0 \\ [\mathbf{J}_{1B}] & [\mathbf{J}_{2B}] & 0 & 0 & 0 \\ 0 & [\mathbf{J}_{2C}] & [\mathbf{J}_{3C}] & 0 & 0 \\ 0 & 0 & [\mathbf{J}_{3D}] & 0 & 0 \\ 0 & 0 & [\mathbf{J}_{3E}] & [\mathbf{J}_{4E}] & 0 \\ 0 & 0 & 0 & [\mathbf{J}_{4F}] & [\mathbf{J}_{5F}] \\ 0 & 0 & 0 & 0 & [\mathbf{J}_{5G}] \end{bmatrix}, [\psi] = \begin{bmatrix} \dot{\varphi}_1^2[\mathbf{A}_1][r_{A1}^{(1)}] \\ \dot{\varphi}_1^2[\mathbf{A}_1][r_{B1}^{(1)}] + \dot{\varphi}_2^2[\mathbf{A}_2][r_{B2}^{(2)}] \\ \dot{\varphi}_2^2[\mathbf{A}_2][r_{C2}^{(2)}] + \dot{\varphi}_3^2[\mathbf{A}_3][r_{C3}^{(3)}] \\ \dot{\varphi}_3^2[\mathbf{A}_3][r_{D3}^{(3)}] \\ \dot{\varphi}_3^2[\mathbf{A}_3][r_{E3}^{(3)}] + \dot{\varphi}_4^2[\mathbf{A}_4][r_{E4}^{(4)}] \\ \dot{\varphi}_4^2[\mathbf{A}_4][r_{F4}^{(4)}] + \dot{\varphi}_5^2[\mathbf{A}_5][r_{F5}^{(5)}] \\ \dot{\varphi}_5^2[\mathbf{A}_5][r_{G5}^{(5)}] \end{bmatrix}. \tag{5}$$

where φ_i is the angle between the local frame's axis x_i and fixed frame x; $[r_{Xi}{}^i]$ are the coordinates vector of point X on body i measured in the local reference frame i; $[A_i]$ is the coordinates transformation matrix, and $[J_{iX}]$ are Jacobian matrix components.

Jacobian matrix components have two lines and three columns given by joint X on the body i, of the form:

$$[\boldsymbol{J}_{iX}] = \begin{bmatrix} 1 & 0 & \mu_a \\ 0 & 1 & \mu_b \end{bmatrix}, \textit{where } [\,\mu_a\ \mu_b\,] = \left[r_X^i\right]^T \begin{bmatrix} 0 & -1 \\ 1 & 0 \end{bmatrix} [\boldsymbol{A}_i], [\boldsymbol{A}_i] = \begin{bmatrix} \cos\varphi_i & -\sin\varphi_i \\ \sin\varphi_i & \cos\varphi_i \end{bmatrix} \tag{6}$$

The differential equations in the general form (3) coupled with the acceleration Eq. (4) constitute a set of [29] *differential-algebraic equations (DAE).* These Eq. (7) contain 29 unknowns: the generalized coordinates and the14 Lagrange multipliers:

https://doi.org/10.1017/S0263574721000345 Published online by Cambridge University Press

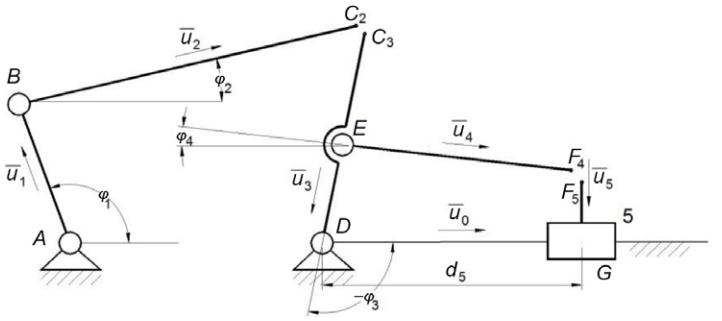


Figure 4. *Open loops of the test mechanism.*

$$\begin{bmatrix} [\mathbf{M}] & [\mathbf{J}]^T \\ [\mathbf{J}] & 0 \end{bmatrix} \begin{bmatrix} \ddot{\mathbf{q}} \\ \lambda \end{bmatrix} = \begin{bmatrix} \mathbf{Q}_{ext} \\ \boldsymbol{\Psi} \end{bmatrix} \tag{7}$$

The system can be solved with different techniques (like coordinate partitioning) or solved as a linear system in the unknown accelerations and Lagrange multipliers, and then integrated for q. In this equation, the constraints are solved at the acceleration level and additional stabilization techniques are required (e.g., Baumgarte stabilization, as shown in Section 6) to assure that are also satisfied at the velocity and displacement level.

3. Models Composed by KCB

In accordance with this model, the mechanism can be seen by a set of KCB interconnected through relative constraints that are distinct from the joints inside the chains. Thus, the mechanism may be a combination of serial chains (having an open-loop structure) or parallel chains (closed-loop structures). This theory [6, 15, 22, 23] is very popular for the development of control algorithms because it enables the direct control of joint movement.

The KCB is the "atomic cell" used for modeling a mechanism and its dof is depending on the number of bodies included in the KCB, in contrast with the MBS case where the "atomic cell" (the body) has a constant number of dof: 3 for the planar motion and 6 for space motion. The terminal body of a KCB is cumulating the degrees of freedom of all the preceding joints [24]. Therefore, the parallel structures can be regarded as a collection of inter-constrained KCBs. The mobility of the mechanism is computed in two steps: first, the mechanical system of rigid bodies is decomposed into individual KCBs (see Fig. 4) by opening a kinematic pair in each closed-loop; second, the mobility is calculated in the same way as for the MBS model – as a sum of KCBs dofs which is reduced by the number of kinematic constraints corresponding to the "opened" joints. Thus, the mobility relationship for the closed-loop system becomes

$$M = \sum f_i - \sum r_i, \tag{8}$$

in which Σf_i is the sum of KCBs degrees of freedom and Σr_i is the number of relative motion limitations introduced by the opened kinematic pair.

Eq. (8) is the equivalent of Gruebler's formula for mechanisms modeled as multi-KCBs. The constraints can be described by algebraic equations, like in the case of the multi-body model. The mobility equation of the KCB model (Eq. (8)) shows that the motion of the mechanism regarded as a set of kinematic chains is defined by a set of kinematic equations.

https://doi.org/10.1017/S0263574721000345 Published online by Cambridge University Press

Lagrange equations enable the dynamic analysis [25]; the DAEs are

$$\begin{cases} \left[\frac{d}{dt}\frac{\partial L}{\partial \dot{\boldsymbol{q}}}\right] - \left[\frac{\partial L}{\partial \boldsymbol{q}}\right] - [\boldsymbol{J}]^T[\lambda] = [\boldsymbol{Q}_{ext}] \\ [\boldsymbol{J}]\,[\ddot{\boldsymbol{q}}] = [\psi] \end{cases} \tag{9}$$

where L is the Lagrangean; the unknowns are the generalized coordinates (in this case the joint angles) and the Lagrange multipliers.

For the test mechanism in Fig. 4, the five generalized coordinates are $[\boldsymbol{q}] = [\,\varphi_1\ \varphi_2\ \varphi_3\ \varphi_4\ d_5\,]^T$. The loop closure constraint equations are reconstructing (closing) the opened kinematic pairs by imposing the coincidence of the pair of points C_2-C_3 and F_4-F_5. The corresponding equations are[12]:

$$\begin{gathered} l_1[u_1] + l_2[u_2] = l_0[u_0] - l_3[u_3] \\ -d_3[u_3] + l_4[u_4] = d_5[u_0] - l_5[u_5], \\ \text{where } [u_0] = \begin{bmatrix} 1 \\ 0 \end{bmatrix}, [u_{1\ldots4}] = \begin{bmatrix} cos\ \varphi_{1\ldots4} \\ sin\ \varphi_{1\ldots4} \end{bmatrix}, [u_5] = \begin{bmatrix} 0 \\ -1 \end{bmatrix}. \end{gathered} \tag{10}$$

Successive differentiation will lead to the following Jacobian matrix and the left-hand side term of the constraint equations:

$$[\boldsymbol{J}] = \begin{bmatrix} -l_1\sin\varphi_1 & -l_2\sin\varphi_2 & -l_3\sin\varphi_3 & 0 & 0 \\ l_1\cos\varphi_1 & l_2\cos\varphi_2 & l_3\cos\varphi_3 & 0 & 0 \\ 0 & 0 & d_3\sin\varphi_3 & -l_4\sin\varphi_4 & 1 \\ 0 & 0 & -d_3\cos\varphi_3 & l_4\cos\varphi_4 & 0 \end{bmatrix} \tag{11}$$

$$[\boldsymbol{\psi}] = \begin{bmatrix} l_1\sin\varphi_1 + l_2\sin\varphi_2 + l_3\sin\varphi_3 \\ l_1\cos\varphi_1 + l_2\cos\varphi_2 + l_3\cos\varphi_3 \\ -d_3\sin\varphi_3 + l_4\sin\varphi_4 \\ -d_3\cos\varphi_3 + l_4\cos\varphi_4 \end{bmatrix} \tag{12}$$

Assuming the potential energy of the system is null (gravity is perpendicular to the motion), the Lagrangean (L) from Eq. (9) is

$$L = \sum E_{ci} = \sum \frac{1}{2} I_i \dot{q}_i^2 + \frac{1}{2} m_i v_i^2 \tag{13}$$

where v_i are the velocities of the center of mass for each body (Fig. 2):

$$\begin{aligned} &\vec{v}_i = \vec{r}_i \times \vec{\omega}_i, \text{ for } i = 1 \text{ and } 3 \\ &\vec{v}_i = \vec{l}_{i-1} \times \vec{\omega}_{i-1} + \vec{r}_i \times \vec{\omega}_i, \text{ for } i = 2 \text{ and } 4 \\ &v_i = \dot{q}_i, \text{ for } i = 5 \end{aligned} \tag{14}$$

After performing the required differentiation, Lagrange's equations of motion (Eq. (9)) take the general form of Eq. (3) in which the mass matrix is not constant and the generalized forces vector is including also velocity-dependent terms, out of the components corresponding to the external forces:

$$[\boldsymbol{M}] = \begin{bmatrix} I_1 + m_1 r_1^2 + m_2 l_1^2 & m_2 l_1 r_2 \cos(\varphi_2 - \varphi_1) & 0 & 0 & 0 \\ m_2 l_1 r_2 \cos(\varphi_2 - \varphi_1) & I_2 + m_2 r_2^2 & 0 & 0 & 0 \\ 0 & 0 & I_3 + m_3 r_3^2 + m_4 d_3^2 & m_4 d_3 r_4 \cos(\varphi_4 - \varphi_3) & 0 \\ 0 & 0 & m_4 d_3 r_4 \cos(\varphi_4 - \varphi_3) & I_4 + m_4 r_4^2 & 0 \\ 0 & 0 & 0 & 0 & m_5 \end{bmatrix} \tag{15}$$

https://doi.org/10.1017/S0263574721000345 Published online by Cambridge University Press

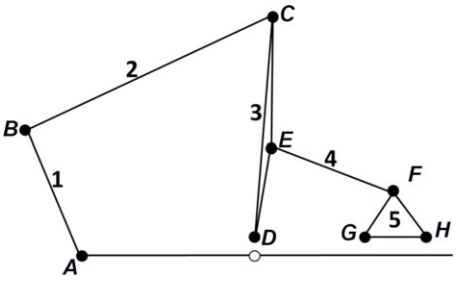


Figure 5. *The KCP model.*

$$[\boldsymbol{Q}_{ext}] = \begin{bmatrix} m_2 l_1 r_2 \omega_2 (\omega_2 - \omega_1)\sin(\varphi_2 - \varphi_1) - m_2 l_1 r_2 \omega_1 \omega_2 \sin(\varphi_2 - \varphi_1) + T_1 \\ m_2 l_1 r_2 \omega_1 (\omega_2 - \omega_1)\sin(\varphi_2 - \varphi_1) + m_2 l_1 r_2 \omega_1 \omega_2 \sin(\varphi_2 - \varphi_1) \\ m_4 d_3 r_4 \omega_4 (\omega_4 - \omega_3)\sin(\varphi_4 - \varphi_3) - m_4 d_3 r_4 \omega_3 \omega_4 \sin(\varphi_4 - \varphi_3) \\ m_4 d_3 r_4 \omega_3 (\omega_4 - \omega_3)\sin(\varphi_4 - \varphi_3) + m_4 d_3 r_4 \omega_3 \omega_4 \sin(\varphi_4 - \varphi_3) \\ -k_{spring}(d_5 - d_{05}) \end{bmatrix} \tag{16}$$

where T_1 is the external torque applied in element 1, k_{spring} is the stiffness of the spring between element 5 and the fixed element, and d_{05} is the free length of the spring.

This model can be solved with a set of *9 DAEs* with 9 unknowns: 5 generalized coordinates and 4 Lagrange multipliers.

4. The KCP Model

Similar to the body models (MBS and KCB models), the particle models are of two categories: MPS models and KCP models. A first formulation in the second category known as "the natural coordinates formulation" was first proposed by de Jalón [5, 26]. Just to facilitate the various joint constraint formulation, out of the mass points, the natural coordinates formulation involves a second type of entity, that is, unit vectors. Similar formulations were proposed later [18, 27].

According to this model, the mechanical system is represented as a collection of chains of basic (or primary) points interconnected through relative motion constraints introduced by the joints. The open chain is formed of points and unit vectors, so two types of generalized coordinates are present in this model: the basic point coordinates and the unit vectors components. The constraint equations express the constant distance between vectors and points, and closing loop constraints like coincidence of points or vectors. Each basic point or unit vector is introducing three generalized coordinates in 3D space called "natural coordinates." For example, in the spatial case two basic (or primary) points of a body are introducing six generalized coordinates from which only five are independent because of the constant distance between the two points.

The test mechanism presented in Fig. 5 has two basic points to model bodies 1, 2, and 4, and three points for body 3 (because of the three joints) and 5 (because of the translational joint). Some of the points are shared between adjacent bodies (*B, C, E,* and *F*). Thus, for this planar mechanism, the generalized coordinates vector has 14 unknowns (the x and y coordinates of these points) for all the 7 mobile basic points in the plane: $\mathbf{q} = [x_A, y_A, x_B, \ldots, y_H]^T$. The kinematic model includes nine equations of the constant distance constraints between the primary points and four for the closing loop constraints introduced by joints D and GH [12]:

$$\begin{aligned} &(x_i - x_j)^2 + (y_i - y_j)^2 - {l_{ij}}^2 = 0, \text{ where } \begin{cases} i = A, B, C, C, D, E, F, F, G \\ j = B, C, D, E, E, F, G, H, H \end{cases} \\ &x_D - l_0 = 0, y_D = y_G = y_H = 0 \end{aligned} \tag{17}$$

https://doi.org/10.1017/S0263574721000345 Published online by Cambridge University Press

The acceleration equations (Eq. (4)) have the following non-zero elements of the Jacobian (a sparse matrix with 13 lines and 14 columns) and right-hand side component:

$$\begin{aligned}
\boldsymbol{J}_{1,1\ldots1,2} &= \left\{ -x_A + x_B,\ -y_A + y_B \right\} \\
\boldsymbol{J}_{2,1\ldots2,4} &= \left\{ x_B - x_C,\ y_B - y_C,\ -x_B + x_C,\ -y_B + y_C \right\} \\
\boldsymbol{J}_{3,3\ldots3,6} &= \left\{ x_C - x_D,\ y_C - y_D,\ -x_C + x_D,\ -y_C + y_D \right\} \\
\boldsymbol{J}_{4,3\ 4,4\ 4,7\ 4,8} &= \left\{ x_C - x_E,\ y_C - y_E,\ -x_C + x_E,\ -y_C + y_E \right\} \\
\boldsymbol{J}_{5,5\ldots5,8} &= \left\{ x_D - x_E,\ y_D - y_E,\ -x_D + x_E,\ -y_D + y_E \right\} \\
\boldsymbol{J}_{6,7\ldots6,10} &= \left\{ x_E - x_F,\ y_E - y_F,\ -x_E + x_F,\ -y_E + y_F \right\} \\
\boldsymbol{J}_{7,9\ldots7,12} &= \left\{ x_F - x_G,\ y_F - y_G,\ -x_F + x_G,\ -y_F + y_G \right\} \\
\boldsymbol{J}_{8,9\ 8,10\ 8,13\ 8,14} &= \left\{ x_F - x_H,\ y_F - y_H,\ -x_F + x_H,\ -y_F + y_H \right\} \\
\boldsymbol{J}_{9,11\ldots9,14} &= \left\{ x_G - x_H,\ y_G - y_H,\ -x_G + x_H,\ -y_G + y_H \right\} \\
\boldsymbol{J}_{10,7} &= 1,\ \boldsymbol{J}_{11,8} = 1,\ \boldsymbol{J}_{12,12} = 1,\ \boldsymbol{J}_{13,14} = 1
\end{aligned} \tag{18}$$

$$[\Psi] = \begin{bmatrix}
\dot{x}_B(\dot{x}_A - \dot{x}_B) + \dot{y}_B(\dot{y}_A - \dot{y}_B) \\
-\dot{x}_B(\dot{x}_B - \dot{x}_C) - \dot{y}_B(\dot{y}_B - \dot{y}_C) + \dot{x}_C(\dot{x}_B - \dot{x}_C) + \dot{y}_C(\dot{y}_B - \dot{y}_C) \\
-\dot{x}_C(\dot{x}_C - \dot{x}_D) - \dot{y}_C(\dot{y}_C - \dot{y}_D) + \dot{x}_D(\dot{x}_C - \dot{x}_D) + \dot{y}_D(\dot{y}_C - \dot{y}_D) \\
-\dot{x}_C(\dot{x}_C - \dot{x}_E) - \dot{y}_C(\dot{y}_C - \dot{y}_E) + \dot{x}_E(\dot{x}_C - \dot{x}_E) + \dot{y}_E(\dot{y}_C - \dot{y}_E) \\
-\dot{x}_D(\dot{x}_D - \dot{x}_E) - \dot{y}_D(\dot{y}_D - \dot{y}_E) + \dot{x}_E(\dot{x}_D - \dot{x}_E) + \dot{y}_E(\dot{y}_D - \dot{y}_E) \\
-\dot{x}_E(\dot{x}_E - \dot{x}_F) - \dot{y}_E(\dot{y}_E - \dot{y}_F) + \dot{x}_F(\dot{x}_E - \dot{x}_F) + \dot{y}_F(\dot{y}_E - \dot{y}_F) \\
-\dot{x}_F(\dot{x}_F - \dot{x}_G) - \dot{y}_F(\dot{y}_F - \dot{y}_G) + \dot{x}_G(\dot{x}_F - \dot{x}_G) + \dot{y}_G(\dot{y}_F - \dot{y}_G) \\
-\dot{x}_F(\dot{x}_F - \dot{x}_H) - \dot{y}_F(\dot{y}_F - \dot{y}_H) + \dot{x}_H(\dot{x}_F - \dot{x}_H) + \dot{y}_H(\dot{y}_F - \dot{y}_H) \\
-\dot{x}_G(\dot{x}_G - \dot{x}_H) - \dot{y}_G(\dot{y}_G - \dot{y}_H) + \dot{x}_H(\dot{x}_G - \dot{x}_H) + \dot{y}_H(\dot{y}_G - \dot{y}_H) \\
0 \\ 0 \\ 0 \\ 0
\end{bmatrix} \tag{19}$$

In case only two basic points are considered for each element (for bodies 3: *B* and *D*, and 5: *G, H*), the mass matrix and Lagrangean have the following components in terms of the generalized coordinates [5]:

$$[\mathbf{M}_i] = \begin{bmatrix}
\frac{m_i}{3} & 0 & \frac{m_i}{6} & 0 \\
0 & \frac{m_i}{3} & 0 & \frac{m_i}{6} \\
\frac{m_i}{6} & 0 & \frac{m_i}{3} & 0 \\
0 & \frac{m_i}{6} & 0 & \frac{m_i}{3}
\end{bmatrix}, \quad \mathrm{i} = 1\ldots5;\ L = \sum_{i=1}^{5} E_{ci} = \frac{1}{2}[\dot{\mathbf{q}}_i]^T[\mathbf{M}_i][\dot{\mathbf{q}}_i] \tag{20}$$

https://doi.org/10.1017/S0263574721000345 Published online by Cambridge University Press

Following the differentiation, the Lagrange equations (Eq. (9)) have the following terms:

$$\left[\frac{d}{dt}\frac{\partial L}{\partial \dot{q}}\right] = \begin{bmatrix} m_1\ddot{x}_A/6 + m_1\ddot{x}_B/3 + m_2\ddot{x}_B/3 + m_2\ddot{x}_C/6 \\ m_1\ddot{y}_A/6 + m_1\ddot{y}_B/3 + m_2\ddot{y}_B/3 + m_2\ddot{y}_C/6 \\ m_2\ddot{x}_B/6 + m_2\ddot{x}_C/3 + m_3\ddot{x}_C/3 + m_3\ddot{x}_D/6 \\ m_2\ddot{y}_B/6 + m_2\ddot{y}_C/3 + m_3\ddot{y}_C/3 + m_3\ddot{y}_D/6 \\ m_3\ddot{x}_C/6 + m_3\ddot{x}_D/3 \\ m_3\ddot{y}_C/6 + m_3\ddot{y}_D/3 \\ m_4\ddot{x}_E/3 + m_4\ddot{x}_F/6 \\ m_4\ddot{y}_E/3 + m_4\ddot{y}_F/6 \\ m_4\ddot{x}_E/6 + m_4\ddot{x}_F/3 \\ m_4\ddot{y}_E/6 + m_4\ddot{y}_F/3 \\ m_5\ddot{x}_G/3 + m_5\ddot{x}_H/6 \\ m_5\ddot{y}_G/3 + m_5\ddot{y}_H/6 \\ m_5\ddot{x}_G/6 + m_5\ddot{x}_H/3 \\ m_5\ddot{y}_G/6 + m_5\ddot{y}_H/3 \end{bmatrix}, \left[\frac{\partial L}{\partial q}\right] = 0 \tag{21}$$

The model for the sample mechanisms can be solved with a set of *27 equations*: 14 differential equations and 13 algebraic constraints. The unknowns are 14 generalized coordinates and 13 Lagrange multipliers.

5. The MPS Model

In 2002, Talaba proposed the particle model for dynamic analysis of MBS [9] and illustrated the use of this model for spatial MBS with flexible bodies [10]. In 2004, Attia published similar models for planar and spatial systems, [8, 11] illustrated in a car suspension rigid mechanism. In the case of the multi-particle model, the mechanism is considered to be a *collection of particles* and they are subject to a set of absolute and relative constraints. Regarding the KCP's formulation, the main difference is that each body of the mechanism is replaced by a set of mass points, but from the inertial point of view, the body is equivalent to the original one. This implies that no adjacent bodies are having "shared" points for joint definition, but the joints are represented as constraints between points of adjacent bodies. In this way, the mechanism is represented as a particle-based model corresponding to each rigid body, having a point contact model for each pair. In the case of the MPS formulation, all joints must be represented by combinations of point constraints (i.e., point-based models) since particles can only have point contact. The various joint models are usually characterized by contact on a surface, on a line or a point.

A set of particles at constant distances are used to model a rigid body, and each particle is associated with an appropriate mass point to maintain inertial equivalence with the original object. MPS formulation is more suitable for use in the study of flexible systems or multiphysics simulations, in which the level of detail goes down often to the point/particle level because it uses geometric data similar to those used in the FEM analysis (particle, nodes). Therefore, selecting the number of particles has two main rules: (i) to select particles needed for the definition of joints and points of interest with respect to the detailed modeling and (ii) to select the minimum possible number of particles to reduce the number of parameters. The position and mass of the particles have to ensure the inertial equivalence with the real body: the centroid position, the axial/centrifugal moments of inertia, and the cumulated mass of the particles. In the case of planar mechanisms, six inertial equivalence equations can be formulated. Thus, a full representation of a planar body could be accomplished using at least two mass points, each of them being characterized by a mass parameter and two Cartesian coordinates. Related to joints, it can

https://doi.org/10.1017/S0263574721000345 Published online by Cambridge University Press

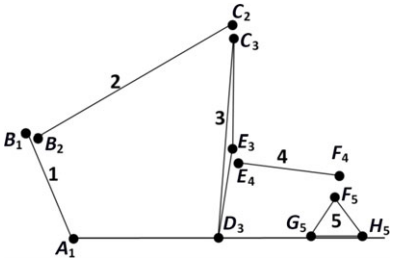


Figure 6. *The multi-particle system (MPS) model.*

be noted that a particle has three degrees of freedom in the 3D space, so the imposed constraints can be the coincidence of two particles, particle in contact with a 3D curve, or particle in contact with a 3D surface.

The test mechanism modeled as MPS system is presented in Fig. 6 and the 2D case was considered. The number of particles is 12: 2 for elements 1, 2, 4 and 3 particles for elements 3 and 5. The generalized coordinates (x and y for each particle) are: $[\mathbf{q}] = [x_{A1}, y_{A1}, x_{B1}, \ldots, y_{H5}]^T$.

The constraints are 9 rigid body constant distances and 14 joint constraints [12]:

$$\begin{cases} (x_{A_1}-x_{B_1})^2+(y_{A_1}-y_{B_1})^2-l_1^2=0 \\ (x_{B_2}-x_{C_2})^2+(y_{B_2}-y_{C_2})^2-l_2^2=0 \\ (x_{C_3}-x_{D_3})^2+(y_{C_3}-y_{D_3})^2-l_3^2=0 \\ (x_{C_3}-x_{E_3})^2+(y_{C_3}-y_{E_3})^2-l_{CE}^2=0 \\ (x_{D_3}-x_{E_3})^2+(y_{D_3}-y_{E_3})^2-l_{DE}^2=0 \\ (x_{E_4}-x_{F_4})^2+(y_{E_4}-y_{F_4})^2-l_4^2=0 \\ (x_{F_5}-x_{G_5})^2+(y_{F_5}-y_{G_5})^2-l_{FG}^2=0 \\ (x_{F_5}-x_{H_5})^2+(y_{F_5}-y_{H_5})^2-l_{FH}^2=0 \\ (x_{G_5}-x_{H_5})^2+(y_{G_5}-y_{H_5})^2-l_{GH}^2=0 \end{cases}, \begin{cases} x_{A_1}-x_{A_0}=0,\ y_{A_1}-y_{A_0}=0 \\ x_{B_2}-x_{B_1}=0,\ y_{B_2}-y_{B_1}=0 \\ x_{C_3}-x_{C_2}=0,\ y_{C_3}-y_{C_2}=0 \\ x_{D_3}-x_{D_0}=0,\ y_{D_3}-y_{D_0}=0 \\ x_{E_4}-x_{E_3}=0,\ y_{E_4}-y_{E_3}=0 \\ x_{F_5}-x_{F_4}=0,\ y_{F_5}-y_{F_4}=0 \\ y_{H_5}=0,\ y_{G_5}=0 \end{cases} \tag{22}$$

Successive differentiation of the position equations will lead to 23×24 Jacobian matrix and left-hand side term in the acceleration equation (J and ψ in Eq. (4)) similar to the KCP method. The only difference is that, due to the joint constraints, there are more non-null elements.

There are reaction, inertia, and external forces acting on the particles, so in the dynamic equations (Eq. (3)) the mass matrix is diagonal, containing the masses of the individual particles ($\mathbf{M}$ = diag[m_{A1}, m_{A1}, m_{B1}, m_{B1}, …, m_{H5}]). There are also joint reaction forces (but no torques) included in Lagrange multipliers and internal reaction forces between body particles.

The MPS model of the test mechanism has *47 equations* with 47 unknown terms: 24 generalized coordinates and 23 Lagrange multipliers.

6. Comparative Simulations

For the formulation of each model, the presented test mechanism was comparatively simulated. In order to ensure the relevance of research, the same conditions have been set regarding the computing power, programming language, as well as numerical data and methods for the mechanism that was subjected to the simulations. All four models were simulated with rigid body assumption with frictionless ideal joints. The equations of motion were formulated using the Newton–Euler's approach, Adams–Moulton–Bashforth solver, and Baumgarte stabilization. The simulation was performed in Matlab, using standardized numerical matrix operations with full and sparse matrices. The code was optimized for

https://doi.org/10.1017/S0263574721000345 Published online by Cambridge University Press

solving the specific models in all cases. The comparison between the efficiency of each model was regarding the run-time and precision, measured with the constraint equation violation.

Adams–Moulton–Bashforth predictor-corrector technique was used as the integration method. This method is using velocity and acceleration values computed in the previous two steps (v_{i-1}, a_{i-1} and v_{i-2}, a_{i-2}). For each integration step, Eq. (7) is solved two times, first for the predicted accelerations (a_{pred}, using the current values of x – generalized positions and v – generalized velocities for each body or point), then for the corrected acceleration ($a_{cor.}$ this time using the predicted values of x and v: $x_{(i+1)p}$ and $v_{(i+1)p}$).

The predicted value of the generalized position and velocities is obtained for each time step i in the following way:

$$v_{(i+1)_p} = v_i + \frac{\Delta t}{12}(23a_{pre.} - 16a_{i-1} + 5a_{i-2}) \tag{23}$$

$$x_{(i+1)_p} = x_i + \frac{\Delta t}{12}(23v_{pre.} - 16v_{i-1} + 5v_{i-2}) \tag{24}$$

The corrected generalized positions and velocities are

$$v_{i+1} = v_i + \frac{\Delta t}{24}(9a_{cor.} + 19a_{pre.} - 5a_{i-1} + a_{i-2}) \tag{25}$$

$$x_{i+1} = x_i + \frac{\Delta t}{24}(9v_{cor.} + 19v_{pre.} - 5v_{i-1} + v_{i-2}) \tag{26}$$

Baumgarte stabilization method was chosen for constraints stabilization. This is a corrective action by adding two terms to the acceleration constraint Eq. (4) [28, 29]. The origin of the method is in the control theory, where the velocity and position constraints are introducing feedback in the equations. The modified acceleration Eq. in (7) can be written as:

$$\Phi_q \ddot{q} = \psi - \alpha(\Phi_q \dot{q} + \Phi_t) - \beta\Phi \tag{27}$$

If α and β coefficients are greater than zero, the equation is stable [28]. These coefficients were selected according to the integration step size [30]:

$$\alpha = \frac{\hat{\alpha}}{\Delta t}, \beta = \frac{\hat{\beta}}{\Delta t^2} \tag{28}$$

where the values selected were $\hat{\alpha} = 0.3$ and $\hat{\beta} = 0.02$, which are inside of the stability region of the characteristic equation [28].

Both the integration step size (10^{-3}s) and the numerical data of the mechanism (see Fig. 2) were kept the same for the simulations based on various models, as follows: $l_0 = 0.12$ m, $l_1 = 0.1$m; $l_2 = 0.165$ m; $l_3 = 0.146$ m; $d_3 = 0.083$ m; $l_4 = 0.217$ m; $l_5 = 0.070$ m; $r_1 = l_1/2$; $r_2 = l_2/2$; $r_3 = d_3$; $r_4 = l_4/2$; $r_5 = l_5/2$; $\varphi_{10} = \pi/2$; $\varphi_{20} = 14°$; $\varphi_{30} = 254.05°$; $\varphi_{40} = 316.33°$: $m_1 = m_2 = m_4 = 0.4$ kg, $m_3 = 0.5$ kg, $m_5 = 0.45$ kg; $I_1 = 1000 + m_1 \cdot l_1^2/2$; $I_2 = 2720 + m_2 \cdot l_2^2/2$; $I_3 = 1822.5 + m_3 \cdot d_3^2/2$; $\omega_1 = \omega_2 = \omega_3 = \omega_4 = v_5 = 0$. The dimensions are fulfilling the Grashof condition for the four-bar mechanisms (the sum of the shortest and longest link is less than the sum of the other two links) for full rotation of the crank.

A torque operating at the level of joint A (T_1=-100 Nm) was considered for the mechanism and the slider was restricted by a spring with k_{spring}=0.012 N/m; d_{05}=0.12 m (free length). Additionally, the modeled mechanism was simulated in MSC ADAMS 2014 [31] using the same input data leading to the validation of the numerical results.

The time history of the obtained displacements and velocities is the same for all cases for the corresponding entities (the four models and the ADAMS model), because of the formulation of the equation of motion with rigid bodies, frictionless connections, and ideal forces. In different modeling methods, the obtained motion is unique if initial conditions for position and velocity are the same and the equations are based on the DAE system [32, 33].

https://doi.org/10.1017/S0263574721000345 Published online by Cambridge University Press

To compare the precision of the four models, the constraints violations were computed as the average values of the constraint equations for each model. In all approaches, the dynamic equations were augmented with the acceleration constraint equations, so constraints violations are present at the position and velocity levels. The source of these is the numerical integration errors [29]. Usually, the reduction of constraint violation is performed with constraint stabilization, coordinate partitioning methods, and direct correct formulations [29]. In this approach, the Adams–Moulton–Bashforth technique and Baumgarte stabilization method were selected and the magnitude of the constraints violations is directly influenced by the chosen integration time step and the penalty parameters.

The time histories of the constraints violations are presented in Fig. 7. These are average values computed over all of the position constraint equations in the four models. It should be highlighted the different time-scale at the beginning of the plot in Fig. 7(a) and the different orders of magnitude. It can be observed that bigger values correspond to the moment when the slider is changing the direction of displacement, but the absolute error in all cases was less than 10^{-3}. The different algorithms used have generally produced similar results, but some differences can still be observed: the average error in the MBS and KCB models is less than 10^{-6} and is smaller than the error of the other two methods. The errors of the third constraint equation in the four models are presented in Fig. 8, but because of the magnitude of them and figure's scale, the MBS and KPC cannot be distinguished. From the computational point of view, all models produce acceptable results [28].

A comparison of the results obtained by the four models is presented in Table 1, and in Fig. 9 the time history of the slider displacement can be seen. The run-time is obtained as the average of 15 simulations in each case. On the same computer, the run-time with ADAMS was 3.15 s.

Following the analysis of the results, some significant issues can be reported:

1. The KCB model is the most effective due to the fact that it results in a significantly lower number of equations (only nine for the case considered).
2. The greater number of equations results in a sparser DAE system.
3. The higher the number of DAEs, the less efficient the model is.
4. The constraint violations are bigger for the particle-based models in comparison to the other two types of models. The computational efficiency would be even worse if a lower level of constraint violation would be imposed.
5. The models with a large number of DAE equations have a very high sparseness value (94.5% for the MPS model of the test mechanism). In the case of the mechanical systems characterized by a large number of differential equations, the sparse matrix techniques could compensate for this disadvantage to some extent, bringing them to more acceptable computational efficiency.

7. Results and Discussion

A comparison was made between the various models. For a given set of numerical data characterizing the considered test mechanism, a simulation was conducted for each mathematical model. The results obtained from these dynamic simulations matched each other numerically with high precision (the absolute error was less than 3×10^{-4} in all cases) and were further verified by a simulation of the same mechanism using ADAMS software. Several features can be outlined for each case:

1. The MBS models allow a simple and intuitive formulation to obtain the equations of motion for MBS. The model can be easily discretized as it is composed of bodies and joints. The system mass matrix is simple to define since its diagonal is composed of the block matrices of individual bodies, while other elements of the mass matrix are null. The mathematical model includes a large set of loosely coupled equations of motion, leading to a sparse associated matrix representation. It is however easy to implement in general-purpose computer programs and achieve good computational efficiency, especially when a sparse matrix numerical implementation is used. The model can be relatively easily enhanced for simulating flexible MBS by integrating modal analysis results at the

https://doi.org/10.1017/S0263574721000345 Published online by Cambridge University Press

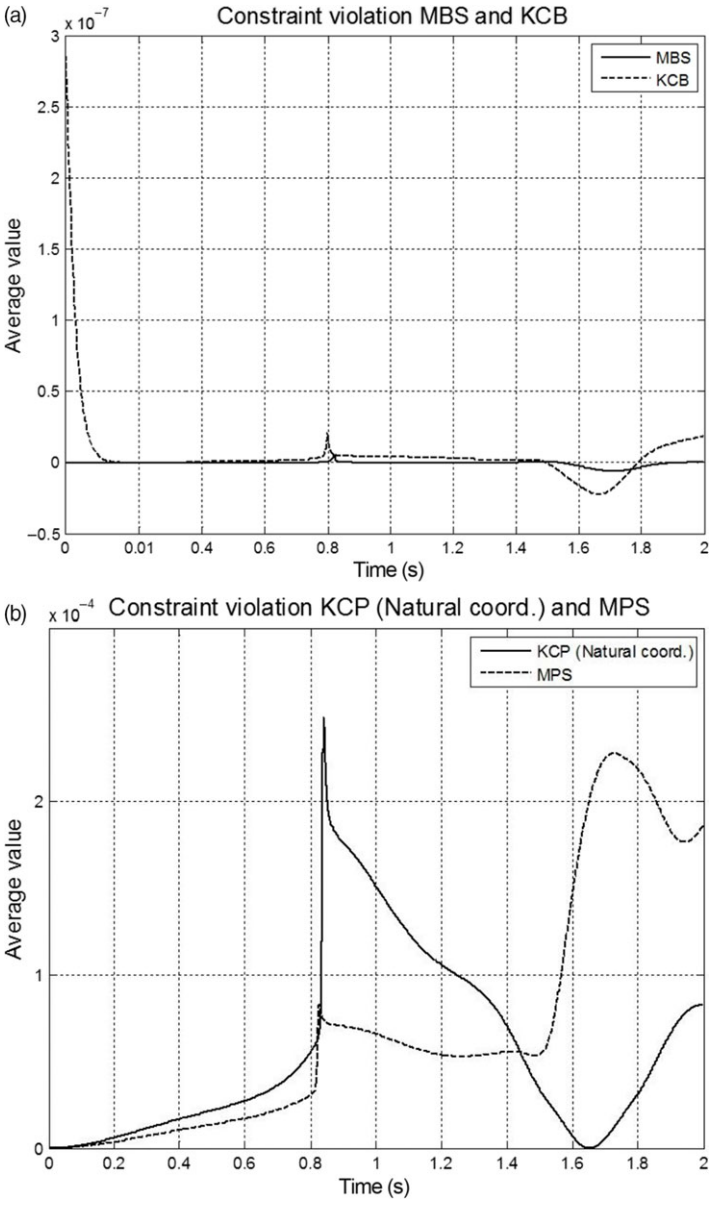


Figure 7. *Average of the constraint violation.*

body level. Several very well-known commercial multi-body programs such as ADAMS and DADS (LMS Virtual.Lab) use this type of formulation.

2. The MPS model is an "imitation" of the MBS model because it uses mass particles instead of bodies as primary entities. The selection of particles for each body must include particles in specific locations needed to define the kinematic joints. It could also include other points of interest, but their number should not be lower than the number required by the static and inertial equivalence with the original rigid bodies. To consider the rigid body conditions, constant distance constraints need to be introduced between the particles for each body. These equations add up to the kinematic constraints leading to the largest set of motion equations among all models and the lowest computational efficiency. However, the model is intuitive and could provide a very detailed discretization

https://doi.org/10.1017/S0263574721000345 Published online by Cambridge University Press

Table 1. *A comparison of the four models..*

Model	Constraint equations (algebraic equations)	Generalized coordinates	Total DAE (differential	DAE matrix sparseness (%) algebraic equations)	Run-time (s)	Real-time comparison (%)
MBS	14	15	29	90.36	6.17	309
KCB	4	5	9	62.96	2.81	140
KCP	13	14	27	86.83	5.89	294
MPS	23	24	47	94.56	9.46	473

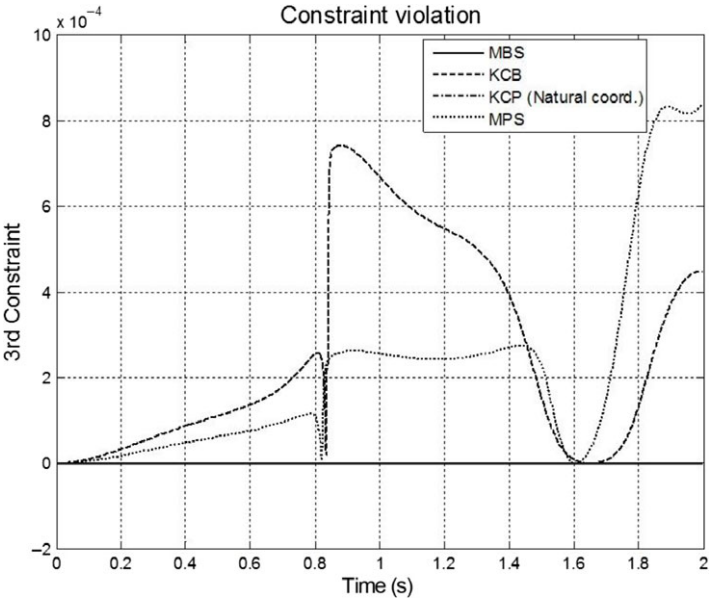


Figure 8. *Errors of the third constraint equations in the models.*

in a specific area of interest, where the model could be additionally developed to include flexible bodies or multiphysics simulations.

3. The kinematic chains models use more complex entities than simple bodies and particles discretizing the mechanism always in serial chains. We identified two types of chains in the literature, that is, (i) chains of bodies and (ii) chains of points (or particles). The mass matrix is variable in all kinematic chains models since the geometrical configuration of the kinematic chain is variable in time and must therefore be recalculated at each integration step. The system discretization is not very simple since there are always several possibilities to define kinematic chains.

Compared to the body and particle-based models, the kinematic chains mathematical models use the smallest number of entities and constraints leading to the smallest possible set of equations of motion and eventually to the best computational efficiency. However, the motion equations involve only Cartesian coordinates and have therefore very simple expressions making the formulation suitable for special-purpose programs that are specific to some particular applications.

The computational efficiency for all four types of models was studied with interesting findings. The research has shown that the models involving less structural entities (i.e., kinematic chain models) lead to a lower number of equations and a higher computational efficiency. Despite leading to a larger number of equations, the models involving more structural entities (MBS and MPS) offer additional features with

https://doi.org/10.1017/S0263574721000345 Published online by Cambridge University Press

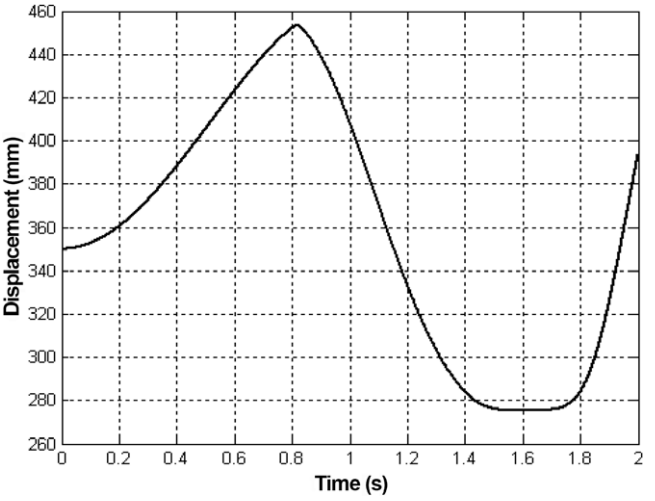


Figure 9. *Displacement of the slider.*

relevance to the non-linear multi-body simulation, providing in-the-loop access for more parameters and are in principle easier to be adapted for a wider range of applications.

8. Conclusions

In this paper, we performed a quantitative assessment of the computational efficiency for various mechanical models. We adopted a physical-based principle for the representation of mechanical systems and this allowed a new classification for the multi-body dynamics formulations known from the literature. Four types of models have been identified: (i) MBS based on bodies, (ii) KCB based on kinematic chains that can include more than one body, (iii) MPS (MPS) models based on particles, and (iv) KCP models that include several particles in every chain. These four mechanical models provide an intuitive context for each case and enable the formulation of different structural criteria for mobility computation and a better evaluation of the mathematical models that are available for analysis.

It has been shown that specific structural formulas indicate for each type of model the number of equations and unknowns for the dynamic analysis of the mechanism. To prove this, well-known and straightforward mathematical formulations have been presented for each model in direct relation with the mechanical structure represented by the respective mobility criteria. A test mechanism was used to illustrate the mathematical model in each case as well as the corresponding numerical solutions.

Acknowledgements. This work was supported by a grant of the Romanian Ministry of Education and Research, CCCDI – UEFISCDI, project number PN-III-P2-2.1-PED-2019-4366 (431PED), within PNCDI III.

Conflicts of Interest. The author(s) declare none.

References

[1] E. Paraskevopoulos and S. Natsiavas, "A new look into the kinematics and dynamics of finite rigid body rotations using Lie group theory," *Int. J. Solids Struct.* **50**(1), 57–72 (2013).
[2] E. J. Haug, "Elements and Methods of Computational Dynamics," **In:** *Computer Aided Analysis and Optimization of Mechanical System Dynamics* (Springer, Berlin, Heidelberg, 1984) pp. 3–38.
[3] E. Haug, *Computer-Aided Kinematics and Dynamics of Mechanical Systems*, (vol. I, Allyn & Bacon, Inc., MA, USA, 1989).
[4] A. A. Shabana, *Dynamics of Multibody Systems* (Cambridge University Press, Cambridge, 2013).
[5] J. García de Jalón and E. Bayo, *Kinematic and Dynamic Simulation of Multibody Systems: the Real Time Challenge* (Springer, Berlin, 1994).

https://doi.org/10.1017/S0263574721000345 Published online by Cambridge University Press

[6] W. O. Schiehlen and E. J. Kreuzer, "Symbolic Computerized Derivation of Equations of Motion," **In:** *Dynamics of Multibody Systems* (K. Magnus ed.) (Springer-Verlag, Berlin, Heidelberg, New York, 1978), pp. 290–305.
[7] W. O. Schiehlen, *Multi-body Systems Handbook* (Springer-Verlag, Berlin, Heidelberg, 1990).
[8] H. A. Attia, "Computational dynamics of three-dimensional closed-chains of rigid bodies," *Appl. Math. Comput.* **172**(1), 286–304 (2006).
[9] D. Talabã, "A Particle Model for Mechanical Systems Simulation: A Model Based Overview of Multi-Body Systems Formulations," **In:** *Virtual Nonlinear Multi-body Systems* (NATO Advanced Study Institute, Prague, 2000) pp. 189–195.
[10] D. Talabã and C. Antonya, "The Multi-Particle System (MPS) Model as a Tool for Simulation of Mechanisms with Rigid and Elastic Bodies," *Proceedings of the 3th International Symposium on Multi-Body Dynamics: Monitoring and Simulation Techniques* (Loughborough, 2004) pp. 111–119.
[11] H. A. Attia, "Equations of motion of planar mechanical systems based on particle dynamics and a recursive algorithm," *Proc. Inst. Mech. Eng. K-J. Multi-Body Dyn.* **218**, 31–38 (2004).
[12] D. Talabã and C. Antonya, "Dynamic Models in Multi-Body Systems," **In:** *Product Engineering: Eco-Design, Technologies and Green Energy* (D. Talaba and T. Roche, eds.) (Springer, Netherlands, 2005) pp. 227–252.
[13] N. Orlandea, M. A. Chace and D. A. Calahan, "A sparsity-oriented approach to the dynamic analysis and design of mechanical system—Part 1," *J. Eng. Ind.* Aug, **99**(3), 773–779 (1977).
[14] P. E. Nikravesh and I. S. Chung, "Application of euler parameters to the dynamic analysis of three-dimensional constrained mechanical systems," *J. Mech. Des.* **104**(4), 785–791 (1981).
[15] J. Wittenburg, *Dynamics of Systems of Rigid Bodies* (Teubner, Stuttgart, 1977).
[16] J. G. De Jalón, J. Unda and A. Avello, "Natural coordinates for the computer analysis of multibody systems," *Comput. Methods Appl. Mech. Eng.* **56**(3), 309–327 (1986).
[17] M. Saura, P. Segado and D. Dopico, "Computational kinematics of multibody systems: Two formulations for a modular approach based on natural coordinates," *Mech. Mach. Theory* **142**(2019), 103602 (2019).
[18] P. E. Nikravesh, *Formulation, Programming with MATLAB§, and Applications* (Taylor & Francis, CRC Press, Boca Raton, 2018).
[19] P. Nikravesh, *Computer-Aided Analysis of Mechanical Systems* (Prentice Hall, Inc., River, NJ, USA, 1988).
[20] P. Flores and H. M. Lankarani, *Contact Force Models for Multibody Dynamics* (Springer International Publishing, Cham, 2016) pp. 53–91.
[21] A. Müller, "Generic mobility of rigid body mechanisms," *Mech. Mach. Theory* **44**(6), 1240–1255 (2009).
[22] R. E. Roberson and R. Schwertassek, *Dynamics of Multi-Body Systems* (Springer Verlag, Berlin, 1988).
[23] T. Huang, S. Yang, M. Wang, T. Sun and D. Chetwynd, "An approach to determining the unknown twist/wrench subspaces of lower mobility serial kinematic chains," *J. Mech. Rob.* **7**(3), 031003 (2015).
[24] D. Talabã, "Mechanical models and the mobility of robots and mechanisms," *Robotica* **33**(1), 1–13 (2014).
[25] E. S. Gebel, "Mathematical modeling of dynamics of multi-lever linkages," *Procedia Eng.* **100**(2015), 1562–1571 (2015).
[26] J. G. de Jalón, "Twenty-five years of natural coordinates," *Multibody Syst. Dyn.* **18**(1), 15–33 (2007).
[27] C. M. Pappalardo, "A natural absolute coordinate formulation for the kinematic and dynamic analysis of rigid multibody systems," *Nonlinear Dyn.* **81**(4), 1841–1869 (2015).
[28] P. Flores, M. Machado, E. Seabra and M. Tavares da Silva, "A parametric study on the Baumgarte stabilization method for forward dynamics of constrained multibody systems," *J. Comput. Nonlinear Dyn.* **6**(1), 011019 (2011).
[29] F. Marques, A. P. Souto and P. Flores, "On the constraints violation in forward dynamics of multibody systems," *Multibody Syst. Dyn.* **39**(4), 385–419 (2017).
[30] S. Lin and J. N. Huang, "Stabilization of Baumgarte's method using the Runge-Kutta approach," *J. Mech. Des.* **124**(4), 633–641 (2002).
[31] M. S. C. ADAMS/ View help – Adams 2014.
[32] L. Yang, S. Xue and W. Yao, "Application of Gauss principle of least constraint in multibody systems with redundant constraints," *Proc. Inst. Mech. Eng. Part K J. Multi-body Dyn.* (2020). doi: 10.1177/1464419320975301
[33] P. Flores, and P. E. Nikravesh, "Comparison of Different Methods to Control Constraints Violation in Forward Multibody Dynamics," *International Design Engineering Technical Conferences and Computers and Information in Engineering Conference*, vol. 55966 (American Society of Mechanical Engineers, 2013) p. V07AT10A028.

Cite this article: Cs. Antonya and R.G. Boboc (2021). "Computational efficiency of multi-body systems dynamic models", Robotica **39**, 2333–2348. https://doi.org/10.1017/S0263574721000345

https://doi.org/10.1017/S0263574721000345 Published online by Cambridge University Press